MEASUREMENT OF THE ZZ PRODUCTION CROSS SECTION IN pp COLLISIONS AT $\sqrt{s} = 13$ TeV WITH THE ATLAS DETECTOR*

Stefan Richter

on behalf of the ATLAS Collaboration

Theoretical Physics Department, CERN, Geneva, Switzerland
and
Department of Physics and Astronomy, University College London
London, United Kingdom

(Received April 12, 2016)

The ZZ production cross section in proton–proton collisions at 13 TeV center-of-mass energy is measured using 3.2 fb^{-1} of data recorded with the ATLAS detector at the Large Hadron Collider. The considered Z boson candidates decay to an electron or muon pair of mass 66–116 GeV. The cross section is measured to be $29.7^{+3.9}_{-3.6}(\text{stat.})^{+1.0}_{-0.8}(\text{syst.})^{+1.7}_{-1.3}(\text{lumi.})$ fb in a fiducial phase space reflecting the detector acceptance. It is also extrapolated to a total phase space for Z bosons in the same mass range and of all decay modes, giving $16.7^{+2.2}_{-2.0}(\text{stat.})^{+0.9}_{-0.7}(\text{syst.})^{+1.0}_{-0.7}(\text{lumi.})$ pb. The results agree with Standard Model predictions. Motivations for the measurement are presented and near-future prospects discussed.

DOI:10.5506/APhysPolB.47.1713

1. Introduction

Studying the production of pairs of Z bosons in proton–proton (pp) interactions at the Large Hadron Collider (LHC) tests the electroweak sector of the Standard Model (SM) at the highest available energies. It also tests quantum chromodynamics (QCD), because higher-order QCD corrections influence the predicted production cross section and jet activity.

Figure 1 shows example Feynman diagrams of two important ZZ production mechanisms in pp collisions at a center-of-mass energy of $\sqrt{s} = 13$ TeV. The production is dominated by quark–antiquark ($q\bar{q}$) interactions (Fig. 1 (a)), with an $\mathcal{O}(10\%)$ contribution from loop-induced gluon–gluon

* Presented at the Cracow Epiphany Conference on the Physics in LHC Run 2, Kraków, Poland, January 7–9, 2016.

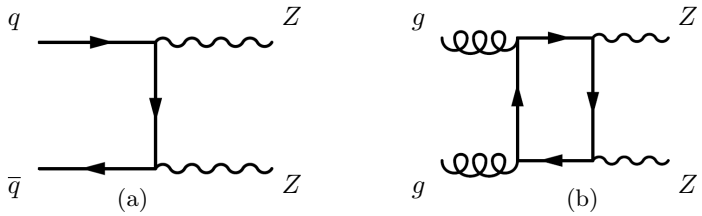

Fig. 1. Example Feynman diagrams for ZZ production initiated by quarks (a) and gluons (b).

(gg) interactions [1, 2] (Fig. 1 (b)). SM ZZ production is also possible via an off-shell Higgs boson propagator. As such, non-Higgs ZZ production is an important background in studies of the Higgs boson [3–5]. It also appears as background in searches for new physics producing pairs of Z bosons at high invariant mass [6, 7], as well as in SM measurements of other diboson processes, such as WZ [8]. Finally, ZZ production is sensitive to triple neutral-gauge-boson couplings, which are not present in the SM [9]. An example Feynman diagram is shown in Fig. 2 (a).

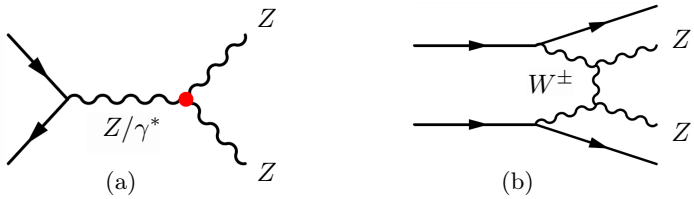

Fig. 2. Example Feynman diagram of ZZ production via triple neutral-gauge-boson coupling, which is absent in the SM (a), and via weak-boson scattering (b).

A possible production channel for ZZ in associated with two jets is weak-boson scattering, of which an example diagram is shown in Fig. 2 (b). This process has a very small cross section and has not yet been observed, but may be within the reach of Run 2 of the LHC (2015–2018).

This note summarizes the results from a recent publication by the ATLAS Collaboration [10], which describes in detail an early measurement of the ZZ production cross section using 3.2 fb^{-1} of data collected with the ATLAS detector [11] at a center-of-mass energy of 13 TeV. Only the inclusive cross section is measured, as not enough data have been collected at this center-of-mass energy to make a meaningful differential cross-section measurement. The presented measurement uses the four-lepton channel, where both Z bosons decay to a pair of either electrons or muons. This gives rise to three signal channels: $4e$, 4μ, and $2e2\mu$. Since a Z boson decaying to charged leptons is not strictly distinguishable from a virtual photon, throughout this note, 'Z boson' refers to the superposition Z/γ^* with mass

66–116 GeV, except in the context of the total cross section extrapolated to all Z boson decay modes. The four-lepton channel has the advantage of having very low background and providing good mass resolution for Z boson candidates. Its disadvantage is a very small branching fraction of less than 0.5% [12], leading to a modest predicted signal cross section of around 70 fb [1]. The measurement is inclusive with respect to additional jet activity. It also includes contributions from double parton scattering.

The ZZ production cross section was previously measured at $\sqrt{s} = 7$ and 8 TeV by the ATLAS and CMS collaborations [13–15] and found to be consistent with SM predictions. ATLAS and CMS also performed a preliminary measurement at 8 TeV and 13 TeV, respectively [16, 17].

2. Early inclusive cross section measurement at 13 TeV

The cross section can be calculated by counting candidate events, subtracting the expected contribution from background events, correcting for detector effects, and dividing by the integrated luminosity. Rather than performing this calculation directly, the result is obtained using a maximum-likelihood estimator in which the signal and background yields are treated as Poisson variables and the systematic uncertainties of the background prediction, correction for detector effects, and integrated luminosity are treated as Gaussian nuisance parameters. The advantage of the maximum-likelihood fit compared to simply using the algebraic formula is a more powerful combination of the three signal channels by fitting simultaneously in all three channels, as well as better propagation of the systematic uncertainty contributions to the uncertainty of the final result.

To minimize model dependence, the cross section is measured in a fiducial region representing the experimental acceptance. In simulated samples, fiducial electrons and muons are required to be prompt, *i.e.* to not originate from hadron or τ decay. To emulate the effects of Bremsstrahlung, the four-momenta of prompt photons within $\Delta R_{\ell,\gamma} = \sqrt{(\Delta\eta_{\ell,\gamma})^2 + (\Delta\phi_{\ell,\gamma})^2} = 0.1$ of a lepton are added to its four-momentum, as motivated in Ref. [18]. The leptons are required to have transverse momentum $p_{\mathrm{T}} > 20$ GeV and pseudo-rapidity $|\eta| < 2.7$. Fiducial events must have exactly four leptons satisfying the above criteria forming two pairs of the same-flavor oppositely charged leptons (e^+e^- or $\mu^+\mu^-$). Each lepton pair must have an invariant mass in the range of 66–116 GeV. In the $4e$ and 4μ channels, where there are two possible ways to form the same-flavor oppositely charged lepton pairs, the combination that minimizes $|m_{\ell\ell,a} - m_Z| + |m_{\ell\ell,b} - m_Z|$ is chosen, where $m_{\ell\ell,a}$ and $m_{\ell\ell,b}$ are the invariant masses of the lepton pairs and m_Z is the pole mass of the Z boson [12]. The distance between any two fiducial leptons must be greater than $\Delta R_{\ell,\ell} = 0.2$.

The selection of reconstructed candidate events is similar to the fiducial selection. Reconstructed electrons [19] and muons [20] are required to have $p_{\mathrm{T}} > 20$ GeV as well as $|\eta| < 2.47$ for electrons and $|\eta| < 2.7$ for muons. The lower $|\eta|$ requirement for reconstructed electrons is due to the more limited experimental acceptance. The small extrapolation up to $|\eta| = 2.7$ for fiducial electrons is considered acceptable, since under the implicit assumption of lepton universality, that area of phase space is still experimentally probed in the channels with muons. By means of impact parameter requirements, the reconstructed leptons are required to originate from the primary vertex of the event, defined as that reconstructed vertex with at least two associated tracks whose associated tracks have the largest sum of squared transverse momenta. They are also required to be isolated from other particles in the detector. Candidate events must satisfy the same selection criteria as fiducial events, with the following additions. The events must have passed a single-muon or dielectron trigger, and each lepton appearing in the trigger must be matched by a selected lepton. Events must have at most one muon without a track in the inner detector or in the muon system.

In the recorded data, a total of 63 events are observed, of which 15, 30, and 18 are in the $4e$, $2e2\mu$, and 4μ channel, respectively.

Two categories of background contributions are considered: backgrounds with four genuine leptons and backgrounds in which there are 1–2 nonprompt or fake leptons (originating from jets or photons). The genuine-lepton background is estimated directly using Monte Carlo (MC) simulation. The background with nonprompt or fake leptons is not modeled well by MC simulation and is, therefore, estimated using control samples and a data-driven technique described in Ref. [13]. The total expected number of background events is 0.20 ± 0.05 ($0.25^{+0.40}_{-0.05}$, $0.17^{+1.00}_{-0.04}$) in the $4e$ ($2e2\mu$, 4μ) channel, giving a total of $0.62^{+1.08}_{-0.11}$ events. This corresponds to only about 1% of the observed number of events. In some channels, the background uncertainty is asymmetric due to truncation, as background contributions cannot be negative.

To allow easy comparison to theoretical predictions, the measured cross section is corrected for detector effects. This is done by dividing it by a correction factor C_{ZZ}, which is determined using MC samples generated with POWHEG + PYTHIA [21–27] and Sherpa [28–34]. Processes are described at next-to-leading order (NLO) in the strong coupling, *i.e.* $\mathcal{O}(\alpha_{\mathrm{s}})$, except for the loop-induced gg-initiated process (Fig. 1 (b)), which only enters at the next-to-next-to-leading order (NNLO), *i.e.* $\mathcal{O}(\alpha_{\mathrm{s}}^2)$, and is described at this order. Its normalization is scaled to $\mathcal{O}(\alpha_{\mathrm{s}}^3)$ accuracy [2]. The C_{ZZ} value and its total uncertainty is determined to be 0.55 ± 0.02 (0.63 ± 0.02, 0.81 ± 0.03) in the $4e$ ($2e2\mu$, 4μ) channel. The values reflect the fact that muons have higher reconstruction efficiency than electrons.

The measured fiducial cross sections are shown in Table I and Fig. 3 along with a comparison to $\mathcal{O}(\alpha_s^2)$ calculations [1]. The predicted cross sections in the fiducial phase space are corrected for QED final-state radiation effects, which amount to a 4% reduction.

TABLE I

Cross-section measurement results compared to the $\mathcal{O}(\alpha_s^2)$ (NNLO) Standard Model predictions. The per-channel and combined fiducial cross sections are shown. For experimental results, the statistical, systematic, and luminosity uncertainties are shown. For theoretical predictions, the PDF and renormalization and factorization scale uncertainties added in quadrature are shown [10].

	Measurement [fb]	$\mathcal{O}(\alpha_s^2)$ prediction [fb]
$\sigma^{\text{fid}}_{ZZ\to e^+e^-e^+e^-}$	$8.4\ ^{+2.4}_{-2.0}(\text{stat.})\ ^{+0.4}_{-0.2}(\text{syst.})\ ^{+0.5}_{-0.3}(\text{lumi.})$	$6.9^{+0.2}_{-0.2}$
$\sigma^{\text{fid}}_{ZZ\to e^+e^-\mu^+\mu^-}$	$14.7\ ^{+2.9}_{-2.5}(\text{stat.})\ ^{+0.6}_{-0.4}(\text{syst.})\ ^{+0.9}_{-0.6}(\text{lumi.})$	$13.6^{+0.4}_{-0.4}$
$\sigma^{\text{fid}}_{ZZ\to \mu^+\mu^-\mu^+\mu^-}$	$6.8\ ^{+1.8}_{-1.5}(\text{stat.})\ ^{+0.3}_{-0.3}(\text{syst.})\ ^{+0.4}_{-0.3}(\text{lumi.})$	$6.9^{+0.2}_{-0.2}$
$\sigma^{\text{fid}}_{ZZ\to \ell^+\ell^-\ell'^+\ell'^-}$	$29.7\ ^{+3.9}_{-3.6}(\text{stat.})\ ^{+1.0}_{-0.8}(\text{syst.})\ ^{+1.7}_{-1.3}(\text{lumi.})$	$27.4^{+0.9}_{-0.8}$

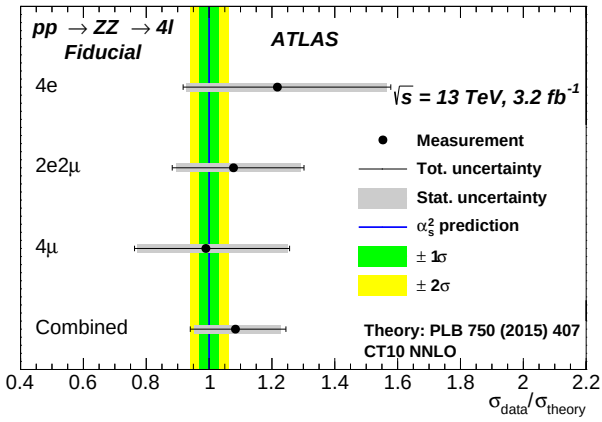

Fig. 3. Comparison between measured fiducial cross sections and $\mathcal{O}(\alpha_s^2)$ predictions [10].

3. Extrapolation to total phase space

For easy comparison to other measurements and calculations where the fiducial definition is different or not implemented, the cross section measured in the fiducial phase space is also extrapolated to the total phase space. The extrapolation factor is obtained from the same combination of MC samples

as used in the C_{ZZ} determination. The ratio of the fiducial to full phase-space cross section is 0.39 ± 0.02, in all three channels. It is corrected for the $\sim 3\%$ increase bias introduced by the pairing algorithm in the $4e$ and 4μ channel. In order to extrapolate to the total cross section, the fiducial cross sections are divided by the ratio 0.39 ± 0.02 and corrected for the leptonic branching fraction $(3.3658\%)^2$ [12]. This value for the branching fraction excludes γ^* contributions. Including these, the branching fraction $ZZ \to \ell^+\ell^-\ell'^+\ell'^-$ is about 1.01–1.02 times larger.

TABLE II

Combined total cross-section result compared to the $\mathcal{O}(\alpha_s^2)$ (NNLO) Standard Model prediction. For the experimental result, the statistical, systematic, and luminosity uncertainty is shown. For theoretical prediction, the PDF and renormalization and factorization scale uncertainty added in quadrature is shown [10].

	Measurement and extrapolation [pb]	$\mathcal{O}(\alpha_s^2)$ prediction [pb]
σ_{ZZ}^{tot}	$16.7\ ^{+2.2}_{-2.0}(\text{stat.})\ ^{+0.9}_{-0.7}(\text{syst.})\ ^{+1.0}_{-0.7}(\text{lumi.})$	$15.6^{+0.4}_{-0.4}$

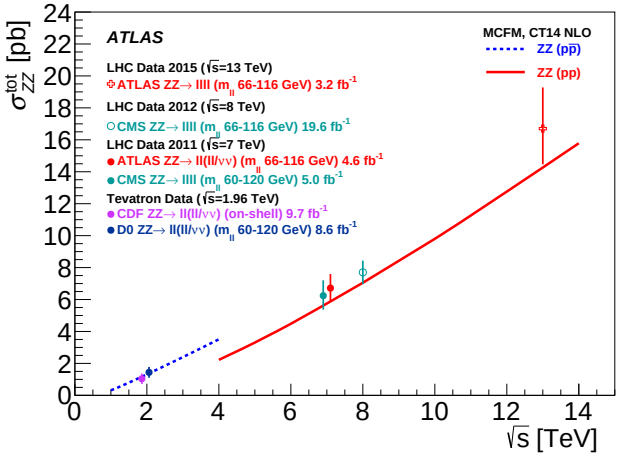

Fig. 4. Total cross section compared to measurements at lower center-of-mass energies by ATLAS, CMS, CDF, and D0 [13–15, 36, 37], and to a prediction from MCFM [35] at $\mathcal{O}(\alpha_s^1)$ accuracy for the $q\bar{q}$-initiated process and at $\mathcal{O}(\alpha_s^2)$ accuracy for the loop-induced gg-initiated process. A full $\mathcal{O}(\alpha_s^2)$ prediction (known to improve agreement at $\sqrt{s} = 13$ TeV) was not yet available for all the different center-of-mass energies. Some data points are shifted horizontally to improve readability [10].

The measured total cross section is shown in Table II. It is compared to measurements at lower center-of-mass energies and to a prediction from MCFM [35], which is calculated at $\mathcal{O}(\alpha_s^1)$ accuracy for the $q\bar{q}$-initiated process and at $\mathcal{O}(\alpha_s^2)$ accuracy for the loop-induced gg-initiated process and is shown *versus* center-of-mass energy in Fig. 4. The cross section increases by a factor of more than two with a center-of-mass energy increase from 8 TeV to 13 TeV.

4. Theoretical aspects

The predictions do not include the following effects. The loop-induced gg-initiated process calculated at $\mathcal{O}(\alpha_s^2)$ could receive large corrections at $\mathcal{O}(\alpha_s^3)$ of 70% [2], which would increase the prediction by 4–5%. Electroweak corrections at next-to-leading order [38, 39] are expected to reduce the cross section by 7–8% [39]. The contribution from double parton scattering is not accounted for in the predictions, but is expected to be an effect of less than 1% [40].

5. Summary

The ATLAS Collaboration has measured the ZZ production cross section in 3.2 fb^{-1} of 13 TeV pp collisions at the LHC using the fully leptonic decay channel $ZZ \to \ell^+\ell^-\ell'^+\ell'^-$. Fiducial cross sections as well as a total cross section for Z bosons with mass 66–116 GeV have been measured and agree well with $\mathcal{O}(\alpha_s^2)$ SM predictions. They agree better with those at $\mathcal{O}(\alpha_s^2)$ (NNLO) than those at $\mathcal{O}(\alpha_s)$ (NLO).

6. Prospects for the near future

In the near future, differential fiducial ZZ cross sections in many variables may be measured and corrected for detector effects. The distributions may be used to search for triple neutral-gauge-boson couplings. The QCD scale uncertainty of the prediction for the gg-initiated process is large [2]. A new measurement of the total cross section with more data to reduce the statistical uncertainty can help constrain this uncertainty. It will also be interesting to study additional jet activity in ZZ events, working towards a search for the weak boson scattering production channel, which is characterized by *tagging jets* (Fig. 2 (b)). This channel allows testing of the SM predictions for the quartic weak boson coupling $WWZZ$.

This work was supported in part by the European Union as part of the FP7 Marie Curie Initial Training Network MCnetITN (PITN-GA-2012-315877).

REFERENCES

[1] M. Grazzini, S. Kallweit, D. Rathlev, *Phys. Lett. B* **750**, 407 (2015).
[2] F. Caola, K. Melnikov, R. Röntsch, L. Tancredi, *Phys. Rev. D* **92**, 094028 (2015).
[3] ATLAS Collaboration, *Phys. Rev. Lett.* **115**, 091801 (2015).
[4] ATLAS Collaboration, *Eur. Phys. J. C* **75**, 335 (2015).
[5] CMS Collaboration, *Phys. Rev. D* **92**, 072010 (2015).
[6] ATLAS Collaboration, `arXiv:1507.00593 [math.CO]`.
[7] CMS Collaboration, *J. High Energy Phys.* **1408**, 174 (2014).
[8] ATLAS Collaboration, `arXiv:1603.00215 [quant-ph]`, submitted to *Phys. Rev. D*.
[9] U. Baur, D.L. Rainwater, *Phys. Rev. D* **62**, 113011 (2000).
[10] ATLAS Collaboration, *Phys. Rev. Lett.* **116**, 101801 (2016).
[11] ATLAS Collaboration, *JINST* **3**, S08003 (2008).
[12] K.A. Olive *et al.*, *Chin. Phys. C* **38**, 090001 (2014).
[13] ATLAS Collaboration, *J. High Energy Phys.* **1303**, 128 (2013).
[14] CMS Collaboration, *Phys. Lett. B* **740**, 250 (2015).
[15] CMS Collaboration, *J. High Energy Phys.* **1301**, 063 (2013).
[16] ATLAS Collaboration, Measurement of the Total ZZ Production Cross Section in Proton–Proton Collisions at $\sqrt{s} = 8$ TeV in 20 fb^{-1} with the ATLAS Detector, Tech. Rep. ATLAS-CONF-2013-020, CERN, 2013.
[17] CMS Collaboration, Measurement of the ZZ Production Cross Section in $\ell\ell\ell'\ell'$ Decays in pp Collisions at $\sqrt{s} = 13$ TeV, Tech. Rep. CMS-PAS-SMP-15-005, CERN, 2015.
[18] ATLAS Collaboration, Proposal for Truth Particle Observable Definitions in Physics Measurements, ATL-PHYS-PUB-2015-013.
[19] ATLAS Collaboration, Electron Efficiency Measurements with the ATLAS Detector Using the 2012 LHC Proton–Proton Collision Data, ATLAS-CONF-2014-032.
[20] ATLAS Collaboration, Muon Reconstruction Performance in Early $\sqrt{s} = 13$ TeV Data, ATL-PHYS-PUB-2015-037.
[21] P. Nason, *J. High Energy Phys.* **0411**, 40 (2004).
[22] S. Frixione, P. Nason, C. Oleari, *J. High Energy Phys.* **0711**, 070 (2007).
[23] S. Alioli, P. Nason, C. Oleari, E. Re, *J. High Energy Phys.* **1006**, 043 (2010).

[24] T. Melia, P. Nason, R. Röntsch, G. Zanderighi, *J. High Energy Phys.* **1111**, 078 (2011).

[25] P. Nason, G. Zanderighi, *Eur. Phys. J. C* **74**, 2702 (2014).

[26] T. Sjöstrand, S. Mrenna, P. Skands, *J. High Energy Phys.* **0605**, 026 (2006).

[27] T. Sjöstrand, S. Mrenna, P. Skands, *Comput. Phys. Commun.* **178**, 852 (2008).

[28] T. Gleisberg *et al.*, *J. High Energy Phys.* **0902**, 007 (2009).

[29] S. Höche, F. Krauss, S. Schumann, F. Siegert, *J. High Energy Phys.* **0905**, 053 (2009).

[30] T. Gleisberg, S. Höche, *J. High Energy Phys.* **0812**, 039 (2008).

[31] S. Schumann, F. Krauss, *J. High Energy Phys.* **0803**, 038 (2008).

[32] M. Schönherr. F. Krauss, *J. High Energy Phys.* **0812**, 018 (2008).

[33] F. Cascioli, P. Maierhöfer, S. Pozzorini, *Phys. Rev. Lett.* **108**, 111601 (2012).

[34] S. Höche, F. Krauss, M. Schönherr, F. Siegert, *J. High Energy Phys.* **1304**, 027 (2013).

[35] J.M. Campbell, R.K. Ellis, *Phys. Rev. D* **60**, 113006 (1999).

[36] T. Aaltonen *et al.* [CDF Collaboration], *Phys. Rev. D* **89**, 112001 (2014).

[37] V.M. Abazov *et al.* [D0 Collaboration], *Phys. Rev. D* **85**, 112005 (2012).

[38] A. Bierweiler, T. Kasprzik, J.H. Kühn, *J. High Energy Phys.* **1312**, 071 (2013).

[39] B. Biedermann *et al.*, `arXiv:1601.00778 [math.NA]`.

[40] ATLAS Collaboration, *New J. Phys.* **15**, 033038 (2013).